0026-895X/11/8005-900–910$25.00
MOLECULAR PHARMACOLOGY
Vol. 80, No. 5
73205/3723390
Mol Pharmacol 80:900–910, 2011
Printed in U.S.A.

TTA-P2 Is a Potent and Selective Blocker of T-Type Calcium Channels in Rat Sensory Neurons and a Novel Antinociceptive Agent

WonJoo Choe, Richard B. Messinger, Emily Leach, Veit-Simon Eckle, Aleksandar Obradovic, Reza Salajegheh, Vesna Jevtovic-Todorovic, and Slobodan M. Todorovic

Department of Anesthesiology, InJe University Ilsan Paik Hospital and College of Medicine, Seoul, Korea (WJ.C.); Departments of Anesthesiology (R.B.M., E.L., A.O., R.S., V.J.-T., S.M.T.) and Neuroscience (V.J.-T., S.M.T.) and Neuroscience Graduate Program (S.M.T., V.J.-T.), University of Virginia Health System, Charlottesville, Virginia; and Department of Anesthesiology and Intensive Care Medicine, Tuebingen University Hospital, Eberhard-Karls University, Tuebingen, Germany (V.-S.E.)

Received April 21, 2011; accepted August 5, 2011

ABSTRACT

Several agents that are preferential T-type calcium (T-channel) blockers have shown promise as being effective in alleviating acute and chronic pain, suggesting an urgent need to identify even more selective and potent T-channel antagonists. We used small, acutely dissociated dorsal root ganglion (DRG) cells of adult rats to study the in vitro effects of 3,5-dichloro-*N*-[1-(2,2-dimethyl-tetrahydro-pyran-4-ylmethyl)-4-fluoro-piperidin-4-ylmethyl]-benzamide (TTA-P2), a derivative of 4-aminomethyl-4-fluoropiperdine, on T currents, as well as other currents known to modulate pain transmission. We found that TTA-P2 potently and reversibly blocked DRG T currents with an IC_{50} of 100 nM and stabilized channel in the inactive state, whereas high-voltage-activated calcium and sodium currents were 100- to 1000-fold less sensitive to channel blocking effects. In in vivo studies, we found that intraperitoneal injections of 5 or 7.5 mg/kg TTA-P2 reduced pain responses in mice in phases 1 and 2 of the formalin test. Furthermore, TTA-P2, at 10 mg/kg i.p., selectively and completely reversed thermal hyperalgesia in diabetic rats treated with streptozocin but had no effect on the nociceptive response of healthy animals. The antihyperalgesic effects of TTA-P2 in diabetic rats were completely abolished by administration of oligonucleotide antisense for $Ca_V3.2$ isoform of T channels. Thus, TTA-P2 is not only the most potent and selective blocker of T channels in sensory neurons yet described, but it also demonstrates the potential for the pharmacological effectiveness of this approach in addressing altered nociceptive responses in animal models of both inflammatory and neuropathic pain.

Introduction

On the basis of the membrane potential at which they gate ion currents, voltage-gated calcium channels are classified as high-voltage-activated (HVA) or sustained currents and low-voltage-activated or transient (T-type) currents (Perez-Reyes, 2003). Different subtypes of HVA currents in the central nervous system (CNS) are important in regulating fast synaptic transmission. In contrast, neuronal T channels have key functions in neuronal membrane oscillations and in lowering the threshold for action potential firing in both the peripheral and central nervous systems. On the basis of cloned sequences of the pore-forming $\alpha 1$ subunit, at least three isoforms of T channels exist: $Ca_V3.1$ ($\alpha 1G$) (Perez-Reyes et al., 1998), $Ca_V3.2$ ($\alpha 1H$) (Cribbs et al., 1998), and $Ca_V3.3$ ($\alpha 1I$) (Lee et al., 1999a). Recent electrophysiological, genetic, molecular, and behavioral studies have suggested that T channels are crucial in controlling the excitability of sensory neurons, act as signal amplifiers, and make a previously unrecognized contribution to both peripheral and central pain processing (Todorovic et al., 2001; Jevtovic-Todoro-

This work was supported by The National Institutes of Health National Institute on Drug Abuse [Grant R21-DA029342]; the Harold Carron Endowment Fund; the American Diabetes Association [Basic Research Grant 7-09-BS-190]; the Department of Anesthesiology at the University of Virginia, InJe University; and a gift from Joseph C. Palumbo and Sandra C. Palumbo.

Article, publication date, and citation information can be found at http://molpharm.aspetjournals.org.

doi:10.1124/mol.111.073205.

ABBREVIATIONS: HVA, high-voltage-activated; DRG, dorsal root ganglion; HEK, human embryonic kidney; PWL, paw withdrawal latency; STZ, streptozocin; TTX, tetrodotoxin; TTA-P2, 3,5-dichloro-*N*-[1-(2,2-dimethyl-tetrahydro-pyran-4-ylmethyl)-4-fluoro-piperidin-4-ylmethyl]-benzamide); ECN, [(3β, 5α, 17β)-17-hydroxyestrane-3-carbonitrile]; CNS, central nervous system; P1, phase 1; P2, phase 2; AS, antisense-$Ca_V3.2$; MIS, Mismatch-$Ca_V3.2$; I-V, current-voltage.

vic and Todorovic, 2006; Snutch and David, 2005; Choi et al., 2007). Furthermore, in vivo experiments showed that use of subtype-specific antisense for knockdown of $Ca_V3.2$ channels in DRG cells completely reversed hyperalgesia in animal models of mechanical injury to the sciatic nerve (Bourinet et al., 2005) and painful diabetic neuropathy (Messinger et al., 2009). This creates interest in further developing pharmacological tools for studies of the function of T channels in pain pathways and for clinical development of specific pain therapies targeting ion channels in sensory neurons.

Although there are many natural toxins or venom components that could be used to study the multiple HVA currents, only recently have substances been identified that are more useful blockers of T currents. Consistent with this, systemic injections of mibefradil, a peripherally acting pan-T-channel blocker (Clozel et al., 1997), suppressed cutaneous, thermal, and mechanical nociception in healthy rats (Todorovic et al., 2002), as well as visceral nociception in healthy mice (Kim et al., 2003). Furthermore, the reversal of symptoms of neuropathic pain associated with chronic constrictive injury of the sciatic nerve has been demonstrated by systemic and local intraplantar injections of mibefradil (Dogrul et al., 2003). Some clinically used antiepileptics such as phenytoin and ethosuximide are in vitro blockers of T channels in sensory neurons (Todorovic and Lingle, 1998) and potent analgesics when injected into peripheral receptive fields of whole animals (Todorovic et al., 2003). It is noteworthy that some other clinically used analgesic drugs target voltage-gated calcium channels. For example, voltage-gated calcium channels are considered a major cellular target for the anticonvulsants gabapentin and pregabalin, which can relieve diabetes-induced neuropathic pain in some populations of patients (Rogawski and Loscher, 2004). However, the use of gabapentin and related drugs is associated with side effects such as excessive sedation in many patients, which necessitates the search for other novel therapies (Edwards et al., 2008).

The usefulness of mibefradil, a prototypical T-channel blocker, has been questioned because recent studies have demonstrated that this molecule, in addition to affecting T channels, can affect several other ion channels, including voltage-gated sodium channels in sensory neurons, with a similar potency (Coste et al., 2007). Likewise, the antiepileptic ethosuximide, another representative T-channel blocker and analgesic in animal pain models (Todorovic et al., 2003), affects T channels and sodium channels in neurons of the CNS with similar potency (Leresche et al., 1998). This raises the question of whether the analgesic effects of these drugs in behavioral pain paradigms can be attributed only to the antagonism of T channels. Thus, despite the progress made in recent years, pharmacological tools for the study of T currents are still very limited [see reviews by McGivern (2006) and Lory and Chemin (2007)], precluding any clinical studies aimed at establishing the potential value of T-channel blockers in treating various pain disorders.

The recent discovery of novel selective T-channel antagonists such as 4-aminomethyl-4-fluoropiperdine is promising because these agents completely block recombinant T-current isoforms with high potency (IC_{50} = 20–100 nM) (Shipe et al., 2008). However, the selectivity, potency, and mechanisms of action of these novel blockers in native cells in pain pathways have not, as yet, been systematically examined. Thus, we hypothesized that one such compound, 3,5-dichloro-*N*-[1-(2,2-dimethyl-tetrahydro-pyran-4-ylmethyl)-4-fluoro-piperidin-4-ylmethyl]-benzamide (TTA-P2; see Fig. 1), may be a potent blocker of native T currents in rat sensory neurons and, accordingly, a useful tool for studies of the role of T channels in pain signaling. To test this hypothesis, we have done biophysical studies using patch-clamp experiments with acutely dissociated sensory neurons of rat dorsal root ganglia and whole-animal behavioral pain experiments with adult rats and mice.

Materials and Methods

Electrophysiological In Vitro Studies

Before the harvest of tissues, rats were deeply anesthetized with isoflurane and rapidly decapitated. For one experiment, we dissected six to eight lumbar dorsal root ganglia from both sides of rats. We prepared acutely dissociated DRG cells and used them within 6 to 8 h for whole-cell recordings as described previously (Todorovic et al., 1998; Nelson et al., 2005, 2007). We focused on small cells (i.e., those with an average soma diameter of 20–30 μm), because functional studies have indicated that most of them are likely polymodal nociceptors belonging to unmyelinated C-type sensory fibers that are capable of responding to noxious mechanical, chemical, and thermal stimuli in vivo (McCleskey and Gold, 1999; Campbell and Meyer, 2006). Our previous studies have confirmed that the majority of acutely dissociated small DRG cells express T currents that are important for control of membrane excitability (Todorovic et al., 1998; Nelson et al., 2005, 2007).

Recordings were made using standard whole-cell techniques. Series resistance (R_s) and capacitance (C_m) values were taken directly from readings of the amplifier after electronic subtraction of the capacitive transients. Series resistance was compensated to the maximum extent possible (usually ~60–80%). In most experiments, we used a P/5 protocol for online leak subtractions. The percentage reductions in peak current at various concentrations of TTA-P2 were used to generate a concentration-response curve. Mean values were fit to the following Hill function:

$$PB([TTA\text{-}P2]) = PB_{max}/(1 + (IC_{50}/[TTA\text{-}P2])^n) \quad (1)$$

where PB_{max} is the maximal percentage block of peak current, IC_{50} is the concentration that produces 50% inhibition, and n is the apparent Hill coefficient for blockade. The fitted value is reported with 95% linear confidence limits. The voltage dependencies of activation and steady-state inactivation were described with single Boltzmann distributions of the following forms.

$$\text{Activation: } G(V) = G_{max}/(1 + \exp[-(V - V_{50})/k]) \quad (2)$$

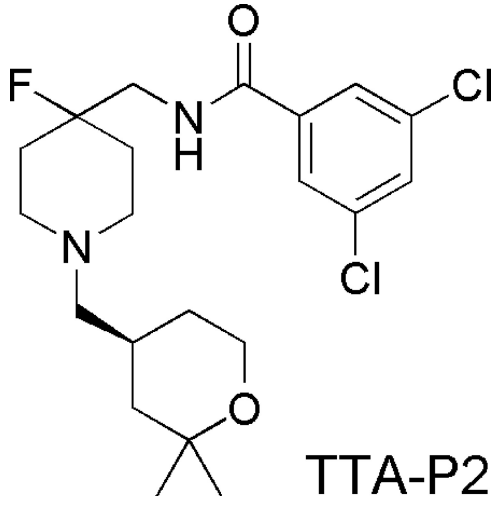

Fig. 1. Structure of TTA-P2 compound evaluated in this study.

$$\text{Inactivation: } I(V) = I_{max}/(1 + \exp[(V - V_{50})/k]) \quad (3)$$

In these forms, I_{max} is the maximal amplitude of current, G_{max} is the maximal conductance, V_{50} is the voltage at which half of the current is activated or inactivated, and k represents the voltage dependence (slope) of the distribution.

The time course of macroscopic T-current inactivation and deactivating tail currents were fitted using a single-exponential equation:

$$y = A_1 \times e^{(-x/\tau 1)} + y_0 \quad (4)$$

where A_1 is the amplitude, τ_1 is the decay constant, and y_0 is the offset.

For fitting the time course of recovery from inactivation, a double-exponential function was used, yielding two time constants ($\tau 1$ and $\tau 2$) and their corresponding amplitudes (A_1 and A_2):

$$y = y0 + A_1 e^{(-x/\tau 1)} + A_2 e^{(-x/\tau 2)} \quad (5)$$

TTA-P2 was prepared as 100- to 300-mM stock solutions in dimethyl sulfoxide. The final concentrations of dimethyl sulfoxide had no significant effect on T-current amplitude in DRG and human embryonic kidney (HEK) 293 cells (data not shown).

The external solution used to isolate T currents contained 2 mM $CaCl_2$, 152 mM TEA-Cl, and 10 mM HEPES adjusted to pH 7.4 with TEA-OH. To minimize contamination of T currents with even minimal HVA components, we used only fluoride (F^-)-based internal solution to facilitate HVA calcium current rundown; this solution contained 135 mM tetramethylammonium hydroxide, 10 mM EGTA, 40 mM HEPES, and 2 mM $MgCl_2$, adjusted to pH 7.2 with hydrofluoric acid. This allowed studies of well isolated and well clamped T currents in small DRG cells. All chemicals were obtained from Sigma-Aldrich (St. Louis, MO) unless noted otherwise. Statistical comparisons were made, where appropriate, using an unpaired Student's t test, Mann-Whitney sum test, and χ^2 test. All quantitative data are expressed as means of multiple experiments ± S.E.M. unless stated otherwise. The amplitude of T current was measured from the peak, which was subtracted from the current at the end of the depolarizing test potential to avoid contamination with residual HVA currents that were present at more positive membrane potentials (typically − 20 mV and higher). To record HVA calcium currents in DRG and HEK cells, we used the same external solution except that equimolar $BaCl_2$ was substituted for $CaCl_2$ and the internal solution contained 110 mM Cs-methane sulfonate, 14 mM phosphocreatine, 10 mM HEPES, 9 mM EGTA, 5 mM Mg-ATP, and 0.3 mM Tris-GTP, adjusted to pH 7.3 with CsOH. For recordings of voltage-gated sodium currents in DRG cells, we used the same fluoride-based internal solution as for recordings of T currents. The external solution contained 140 mM NaCl, 4 mM KCl, 2 mM $MgCl_2$, 2 mM $CaCl_2$, 0.5 mM $CdCl_2$, 10 mM glucose, and 10 mM HEPES, adjusted to pH 7.4. In some experiments, this solution was supplemented with 1 μM tetrodotoxin (TTX).

In Vivo Studies

Chemicals and Animals. In all experiments, Sprague-Dawley adult female rats (retired breeders) and adult C57BL/6 mice of both sexes were used. Streptozocin (STZ) was purchased from Sigma-Aldrich. Antisense oligonucleotides and mismatched oligonucleotides [using the sequence previously published by Bourinet et al. (2005); Messinger et al., 2009] were purchased from Invitrogen (Carlsbad, CA). Antisense-$Ca_V3.2$ (AS) (CCACCTTCTTACGCCAGCGG), which was used to knock down the T-type-channel pore-forming subunit of the gene encoding the α1H ($Ca_V3.2$) or Mismatch-$Ca_V3.2$ (Mis-$Ca_V3.2$; MIS) (TACTGTACTTGCGAGGCCAC) were dissolved in sterile neutral pH buffer solution. Vehicle experiments were performed using sterile saline neutral pH buffer solution. As in previous studies (Messinger et al., 2009), vehicle and MIS were found to have no effect on thermal nociception.

TTA-P2 was kindly provided by Drs. John Renger and Victor N. Uebele (Merck Research Laboratories, West Point, PA). For all of our in vivo studies TTA-P2 was dissolved in 15% cyclodextrin and injected intraperitoneally at the doses of 5, 7.5, or 10 mg/kg. Cyclodextrin [(2-hydroxypropyl)-β-cyclodextrin] solution (Sigma-Aldrich) was balanced at pH 7.4 just before injection.

Induction of Peripheral Diabetic Neuropathy with Streptozocin. All experimental protocols were approved by the University of Virginia Animal Care and Use Committee and were in accordance with the *Guide for the Care and Use of Laboratory Animals* (Institute of Laboratory Animal Resources, 1996). All possible efforts were made to minimize animals' suffering and to minimize the number of animals used.

To induce peripheral diabetic neuropathy, we intravenously injected freshly dissolved STZ solution at pH 5 to 6, using a dose of 50 mg/kg. This dose causes severe hyperglycemia and pain-like behavior within the first few days after injection but does not cause severe generalized sickness (e.g., ketoacidosis, malaise, wasting) (Aley and Levine, 2001; Jagodic et al., 2007; Messinger et al., 2009). Control rats received the same volume per kilogram of intravenous sterile saline. The animals were studied for 10 days after the day of intravenous injection.

Three days after injecting STZ (or saline), at which point STZ-injected rats had developed peripheral diabetic neuropathy, we intrathecally injected 12.5 μg/25 μl of either AS or MIS (or 25 μl of saline) into the L_{5-6} region of the spinal cord every 12 h for 4 days (a total of eight injections) to test the effects of oligonucleotides. All solutions were pH balanced to 7.4 to avoid spinal cord irritation. Rats were maintained in a surgical plane of anesthesia with isoflurane (2–3% in oxygen delivered via nose cone) throughout the injection procedure. We previously showed that intrathecal injections as described lead to preferential uptake of AS by DRG sensory neurons and minimal uptake by spinal cord tissues (Messinger et al., 2009). This method of AS application reliably reversed neuropathic hyperalgesia in diabetic rats and concomitantly reversed up-regulation of T currents in rat sensory neurons, whereas injections of saline or MIS intrathecally in the same manner did not affect pain responses and T-current density in DRG cells (Messinger et al., 2009).

Behavioral Studies

Assessment of Thermal Sensitivity. The nociceptive response to thermal stimulation was measured using a paw thermal stimulation system consisting of a clear plastic chamber (10 × 20 × 24 cm) that sits on a clear elevated glass floor and is temperature regulated at 30°C. As described previously (Messinger et al., 2009), each rat is placed in the plastic chamber for 15 min to acclimate. A radiant heat source mounted on a movable holder beneath the glass floor is positioned to deliver a thermal stimulus to the plantar side of the hind paw. When the rat withdraws the paw, a photocell detects interruption of a light-beam reflection, and the automatic timer shuts off. This method has a precision of ±0.05 s for the measurement of paw withdrawal latency (PWL). To prevent thermal injury, the light beam is automatically discontinued at 20 s if the rat fails to withdraw its paw. Pain testing was done before STZ or vehicle injection (day 0) and daily thereafter for up to 10 days. The stability of daily pain recordings was confirmed by saline-injected controls.

Statistical Analysis. PWLs were subjected to analysis of variance containing one within-subject variable, test session (before the administration of STZ or vehicle versus each post-treatment day up to 10 days), and one between-subject variable, AS versus TTA-P2. Relevant pairwise comparisons were done, and α levels were adjusted using the Bonferroni procedure when appropriate.

Assessment of Inflammatory Pain in Mice. Behavioral tests for inflammatory pain after formalin injection were done with mice in a clear Plexiglas chamber prefilled with air at a flow of 6 l/min, as we reported recently (Orestes et al., 2011). Each mouse was first placed in the prefilled chamber to accommodate for 30 min and then removed from the chamber, injected in the plantar side of the right paw with 20 μl of 5% formalin or vehicle (15% cyclodextrin), and returned to the test chamber. The time in seconds that the mouse

spent licking and biting the paw was measured for 1 h and recorded per every 5-min interval. Afterward, the mouse's temperature was measured to ensure normothermia. To test the effects of TTA-P2, a mouse was injected intraperitoneally with fresh TTA-P2 solution (5 or 7.5 mg/kg) or an equal volume of vehicle. Thirty minutes later, the mouse was placed inside the chamber to equilibrate and become familiar with the environment. One hour after the injection of TTA-P2 or vehicle, the mouse was given an injection of formalin. The rest of the experiment was performed as described in the preceding section.

Assessment of Sensorimotor Abilities. The sensorimotor battery in mice consisted of three tests: ledge, platform, and inclined screen. These tests are designed to assess agility and fine motor abilities, as we described in a recent publication (Latham et al., 2009).

Results

The in vitro results presented here were obtained from a total of 144 small DRG cells having an average soma diameter of 25 ± 3 μm (mean ± S.D.) and an average membrane capacitance of 24 ± 4 pF (mean ± S.D.). We began our study by testing the effects of TTA-P2 on well isolated T currents in rat sensory neurons. Traces (Fig. 2A) and time course (Fig. 2B) from the same representative DRG cell indicate that at 1 μM, TTA-P2 inhibited most of the T current that was recorded at holding potentials (V_h) of − 90 mV. Figure 2B shows that the inhibitory effect of TTA-P2 had a fast onset but was slowly and only partially reversible. Interestingly, similarly fast onset and slow reversibility of the inhibition of T currents with TTA-P2 in thalamic relay neurons has also been reported (Dreyfus et al., 2010). Furthermore, the traces shown in Fig. 2C demonstrate that TTA-P2 at 10 μM had little effect (less than 10%) on the amplitude of HVA Ca^{2+} currents in acutely dissociated DRG cells. For recordings of HVA currents, cells were held at − 50 mV to separate that signal from T currents that are almost completely inactivated at positive membrane potentials.

Some of the calcium channel blockers thought to be selective for T currents (e.g., mibefradil, nickel, ethosuximide) may also affect the *R*-type ($Ca_V2.3$) subtype of HVA calcium currents in the same concentration range (Randall and Tsien, 1997; Nakashima et al., 1998). The above studies have also shown that separation of T currents from *R*-type currents in native cells is further complicated by the fact that they appear to inactivate at somewhat comparable rates. Thus, we tested the ability of TTA-P2 to inhibit human recombinant $Ca_V2.3$ channels stably coexpressed with β3 calcium channel subunits in HEK 293 cells (Nakashima et al., 1998). Traces from a representative HEK 293 cell shown in Fig. 2D demonstrate that TTA-P2 at 10 μM inhibited only approximately 10% of the recombinant $Ca_V2.3$ current. We also tested the ability of TTA-P2 to inhibit voltage-gated sodium currents (I_{Na+}), because these channels are critical

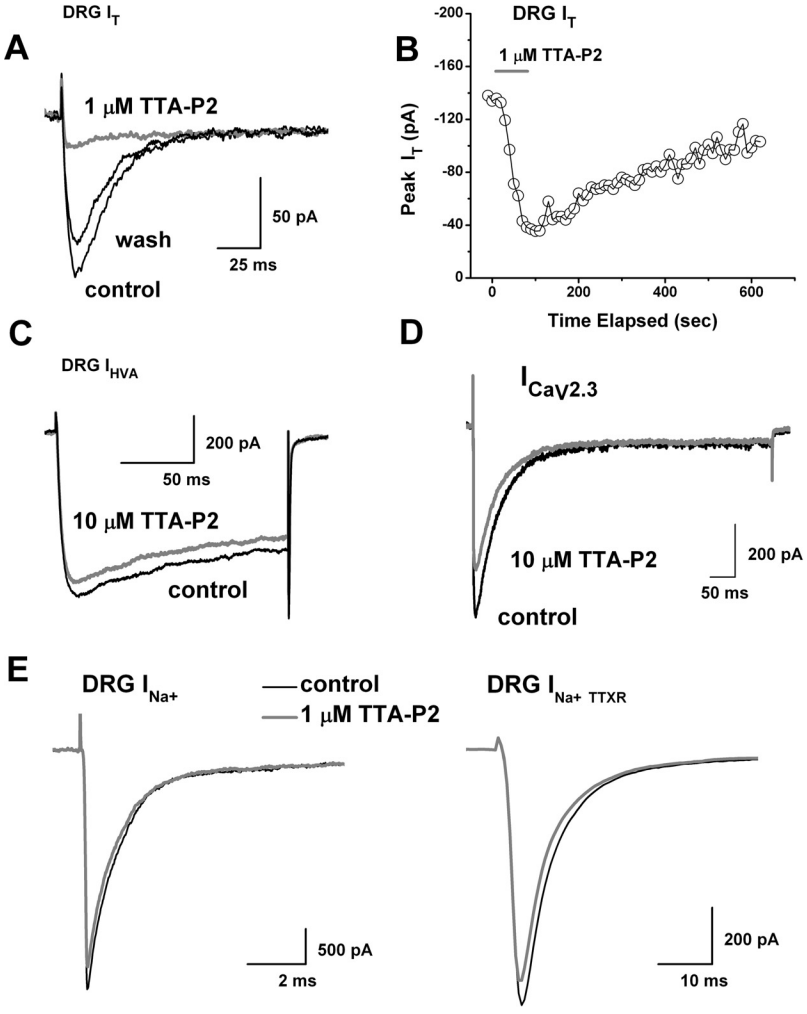

Fig. 2. TTA-P2 selectively inhibits T currents in acutely dissociated adult rat sensory neurons. A, traces of T current in a representative DRG cell before and after (black traces) and during (gray trace) bath application of 1 μM TTA-P2, which reversibly inhibited most of the peak inward current. Currents were evoked from a holding potential (V_h) of − 90 mV and stepping to test potential (V_t) of − 30 mV. Bars indicate calibration. B, temporal record from the same cell presented in A. The gray bar indicates duration of TTA-P2 application. C, traces of HVA current from another DRG cell before (black trace) and during (gray trace) the bath application of 10 μM TTA-P2. TTA-P2 inhibited less than 10% of peak current. Currents were evoked from V_h of − 50 mV and stepping to V_t of − 10 mV. Bars indicate calibration. D, traces of recombinant $Ca_V2.3$ current from a representative HEK 293 cell before (black trace) and during (gray trace) the bath application of 10 μM TTA-P2, which inhibited approximately 20% of the peak current. Currents were evoked from V_h of − 80 mV and stepping to V_t of − 20 mV. Bars indicate calibration. E, traces of total sodium current (I_{Na+}) from a representative DRG cell are shown on the left. Traces of TTX-resistant sodium current ($I_{Na+\ TTXR}$) from another DRG cell are presented on the right. Note that there is little difference between baseline current (black traces) and during the bath application (gray traces) of 1 μM TTA-P2. Currents are evoked from V_h of − 90 mV and stepping to V_t of − 20 mV. Bars indicate calibration.

regulators of the excitability of nociceptive sensory neurons and are implicated in neuropathic pain (Dib-Hajj et al., 1999; Lai et al., 2002; Hong et al., 2004). Traces from representative DRG cells shown in Fig. 2E demonstrate that 1 μM TTA-P2 had little effect on the amplitude of total voltage-gated sodium currents (Fig. 2E, left, I_{Na+}) or the tetrodoxin-resistant component of voltage-gated sodium currents (Fig. 2E, right, $I_{Na+TTXR}$). On average, the effects of 1 μM TTA-P2 on the amplitude of DRG sodium currents were as follows: total I_{Na+}, 1 ± 4% change ($p > 0.05$, $n = 8$); $I_{Na+TTXR}$, 1 ± 7% change ($p > 0.05$, $n = 5$). To compare the potency of TTA-P2 in inhibiting T currents and HVA currents in DRG cells, as well as recombinant $Ca_V2.3$ currents, we obtained multiple points on concentration-response relationships and generated best fits using eq. 1 (Fig. 3). These experiments indicated, impressively, that TTA-P2 was 2 to 3 orders of magnitude more potent in inhibiting DRG T currents (Fig. 3, filled circles; $IC_{50} = \sim$100 nM) than it was in inhibiting total DRG HVA currents (Fig. 3, filled squares; $IC_{50} = \sim$165 μM) and recombinant $Ca_V2.3$ currents (Fig. 3, open triangles; $IC_{50} = \sim$35 μM).

We then set out to discern the biophysical mechanisms of T-current inhibition by TTA-P2, which could contribute to the inhibition of current and, consequently, diminish the cellular excitability of DRG cells. To determine the effects of TTA-P2 on the kinetic properties of DRG T currents, we measured current-voltage (I-V) relationships in the presence and absence of 0.1 μM TTA-P2 ((Fig. 4A), finding that, compared with controls (open symbols), TTA-P2 (filled symbols) reduced T-current amplitudes at all test potentials between − 50 and − 20 mV (Fig. 4B) but had little effect on the kinetics of macroscopic current inactivation (Fig. 4C) or activation (Fig. 4D). The only significant effect was that

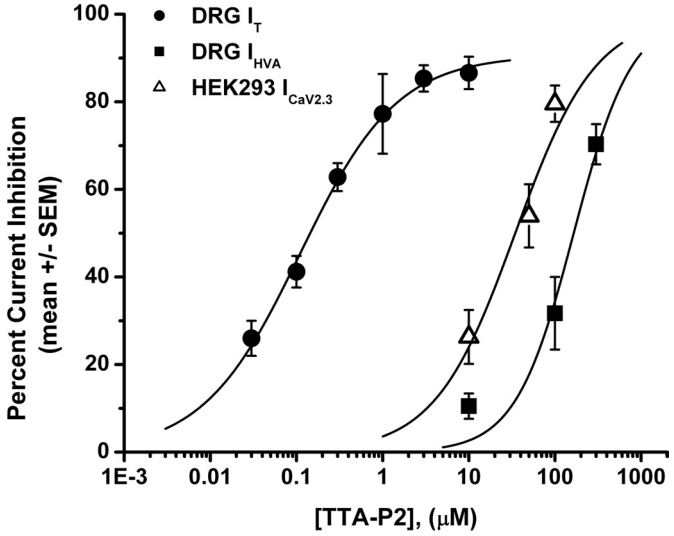

Fig. 3. TTA-P2 inhibits T currents in DRG cells more potently than it does HVA currents in DRG cells and recombinant $Ca_V2.3$ currents in HEK 293 cells. The graphs illustrate concentration-response relationships for TTA-P2 inhibition of T currents in rat DRG cells (filled circles), HVA currents in DRG cells (filled squares), and recombinant $Ca_V2.3$ currents in HEK 293 cells (open triangles) ($n = 4$–15 cells per data point). The solid line is the best fit (eq. 1; see *Materials and Methods*) for T-current inhibition ($IC_{50} = 0.11 \pm 0.01$ μM; slope coefficient, 0.8 ± 0.1; maximal inhibition, 90 ± 3% of the peak current), HVA current inhibition ($IC_{50} = 165 \pm 35$ μM; slope coefficient, 1.3 ± 0.5; maximal inhibition constrained to 100%), and $Ca_V2.3$ current inhibition ($IC_{50} = 35 \pm 9$ μM; slope coefficient, 0.9 ± 0.3; maximal inhibition constrained to 100%).

TTA-P2 slowed 10 to 90% rise time at test potential of − 40 mV for approximately 50% (Fig. 4D). Likewise, TTA-P2 did not induce significant alterations of channel gating, as shown by similar half-maximal activation (V_{50}) of the T channels before and during drug application (Fig. 4E). It is worth noting that TTA-P2 decreased the rate of channel closure after repolarization, as demonstrated by significantly slower deactivation time constants (τ values) at − 130, − 120, − 110, and − 100 mV (Fig. 4F). Binding to inactivated states and off rate of the compound are important properties of drugs that modulate ion channels because it allows them to have tissue selectivity based on the different membrane potential cycling conditions. Transitions from closed to inactivated states can be measured using long prepulses at different potentials, producing what are commonly referred to as steady-state inactivation curves. We assessed steady-state inactivation curves using a standard double-pulse protocol with 3.6-s-long prepulses to variable voltages (from − 110 to − 45 mV) and test potentials to − 30 mV. As shown in Fig. 5, A and B, TTA-P2 (filled symbols), compared with control conditions (open symbols), had a great effect on the voltage-dependent kinetics of channel inactivation, as determined by a hyperpolarizing shift in steady-state inactivation curves of approximately 20 mV. These data suggest that TTA-P2 binds to and stabilizes inactive states of the channel and thus is a more potent blocker at depolarized membrane potentials. For example, it is evident in Fig. 5A that 100 nM TTA-P2 inhibits approximately 40% of maximal T current at − 110 mV, whereas the same concentration inhibits T current almost 100% at − 65 and − 60 mV. T channels can recover from inactivation during sufficiently long hyperpolarizations of the neuronal membrane caused by the effects of neuromodulators such as serotonin in DRG neurons (Nelson et al., 2005). This can drastically influence firing properties of cells that express T channels. Thus, we studied the effects of 100 nM TTA-P2 on recovery from inactivation using our standard double-pulse protocol with variable interpulse duration at − 90 mV (Fig. 5C) after a 500-ms-long inactivating pulse ($V_h = -90$ mV; $V_t = -30$ mV). Figure 5C depicts these data indicating that in the presence of TTA-P2 (filled squares), T currents recover partially to only approximately 60% of the T-current amplitudes of predrug control values (Fig. 5C, open circles). The hyperpolarizing shift in steady-state inactivation and incomplete recovery from inactivation could be highly useful properties for a channel inhibitor because, when applied in vivo, it will affect actively firing neurons more potently than it will resting cells. Thus, we tested the efficacy of TTA-P2 in two frequently used animal models of pain.

Previous studies with $Ca_V3.2$ knockout mice have established the role of T channels in inflammatory pain (Choi et al., 2007). Thus, to explore the interaction of TTA-P2 and T channels in vivo, we used injections of formalin into the hind paws of mice to measure inflammatory pain. The amount of time mice spend licking and biting the injected paw in the first 5 min after injection is a response to direct activation of peripheral nociceptors [phase 1 (P1)]. In contrast, responses 10 to 60 min after injection reflect central sensitization of pain [phase 2 (P2)]. As shown in Fig. 6A, TTA-P2 at 7.5 mg/kg i.p. (gray bars), compared with vehicle controls (black bars), significantly reduced licking and biting of the affected paws in P1, P2, and total time from 30 to 50%. When TTA-P2 was injected at a dose of 5 mg/kg i.p., mice demonstrated somewhat reduced, but not significant (approximately 20%), an-

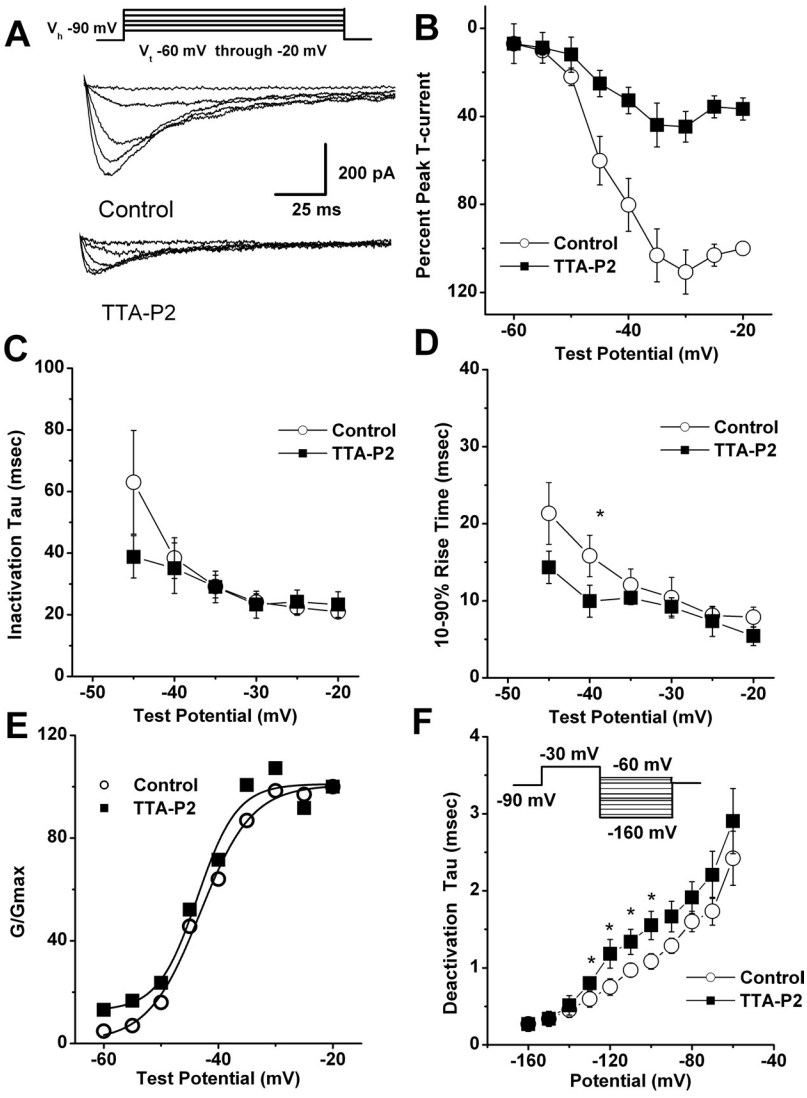

Fig. 4. The effects of TTA-P2 on kinetic properties of T currents in rat DRG cells. A, traces represent families of averaged T currents evoked in the same DRG cells ($n = 5$) in control conditions (top) and during application of 100 nM TTA-P2 (bottom) by voltage steps from − 90 mV (V_h) to V_t from − 60 to − 20 mV in 10-mV increments. Bars indicate calibration. Inset, voltage-clamp protocol used to elicit currents. B, average I-V curves are shown from the same DRG cells shown in A before (open symbols) and during (filled symbols) bath application of 100 nM TTA-P2 using voltage steps in 5-mV increments. Note that TTA-P2 depressed the amplitude of T current similarly at most test potentials. C and D, we measured time-dependent activation (10–90% rise time; D) and inactivation τ (single-exponential fit of decaying portion of the current waveforms using eq. 4; C) from I-V curves in DRG cells shown in B over the range of test potentials from − 45 to − 20 mV. There are few differences between the control (open symbols) and TTA-P2 (filled symbols) groups with the exception of the 10–90% rise time at − 40 mV (D). *, $p < 0.05$. E, data points for channel conductance (G) are calculated from the graph presented in B by dividing current amplitudes with the driving force for ion permeation. Estimated reversal potential was taken to be 60 mV. Solid lines are fitted using eq. 2 (see *Materials and Methods*), giving half-maximal conductance (V_{50}), which occurred at − 43.2 ± 0.6 mV with a slope k of 4.5 ± 0.6 mV in control conditions (open symbols). Likewise, V_{50} was − 43.6 ± 0.3 mV with a k of 3.5 ± 1.0 mV during TTA-P2 application (filled symbols). F, deactivating tail currents in controls (open symbols) and during application (filled symbols) of 100 nM TTA-P2 were fit with a single-exponential function. The resulting τ values are plotted ($n = 5$ cells). Points that are statistically significant are marked with an asterisk ($p < 0.05$). Inset, voltage-clamp protocol. Vertical lines in B–D and F represent S.E.M. of multiple determinations.

algesia in P1, whereas total time and P2 were significantly decreased by approximately 50% (Fig. 6A, open bars).

We also considered the possibility that TTA-P2 might nonspecifically decrease pain responses by inducing a general depression of behavioral performance. To determine whether TTA-P2, given at its effective analgesic doses in mice of 5 or 7.5 mg/kg, causes sensorimotor disturbances such as motor weakness or sedation, which could affect the validity of behavioral sensory testing, we did a battery of sensorimotor tests focused on agility and fine motor abilities (Latham et al., 2009). Mice were tested using an inclined plane (Fig. 6B, left), platform (Fig. 6B, middle), and ledge (Fig. 6B, right) before TTA-P2 injection and at 60 min after injection. The responses of mice treated with 5 mg/kg TTA-P2 (Fig. 6B, open bars) or 7.5 mg/kg TTA-P2 (Fig. 6B, gray bars) did not significantly differ from these mice's responses before injection (Fig. 6B, black bars) on any of the tests, indicating that the effect of TTA-P2 on alleviation of inflammatory pain is unlikely to result from sedation or motor impairment.

Our recent studies have established that T channels are up-regulated in putative nociceptive sensory neurons of diabetic rats treated with STZ and that this up-regulation may increase the cellular excitability of these neurons (Jagodic et al., 2007). Furthermore, we used specific in vivo knockdown of the most prevalent isoform of T channels in DRG sensory neurons, $Ca_V3.2$, to alleviate neuropathic pain in STZ-treated diabetic rats (Messinger et al., 2009). We first asked whether pharmacological antagonism of T channels with TTA-P2 could reverse thermal hypersensitivity in diabetic rats treated with STZ. As shown in Fig. 7 (top), incremental doses of TTA-P2 at 5, 7.5, or 10 mg/kg did not change baseline pain responses (B) in either right paws (open symbols) or left paws (filled symbols) of control animals. When the same doses of TTA-P2 were injected into diabetic STZ-treated rats with neuropathic hyperalgesia as demonstrated by an approximate 30% reduction in thermal PWLs, there was progressive alleviation of pain (Fig. 7, middle). At 10 mg/kg TTA-P2 i.p., there was a complete reversal of neuropathic hyperalgesia as demonstrated by apparent normalization of thermal PWLs. In control experiments, the same volume of vehicle injected into diabetic rats intraperitoneally did not significantly affect PWLs: right-paw controls, 6.9 ± 1.3 s; vehicle, 6.9 ± 0.4 s; left-paw controls, 7.6 ± 2.3 s; vehicle, 6.5 ± 0.5 s ($p > 0.5$, $n = 3$; data not shown). We next asked whether the efficacy of TTA-P2 could be mediated by off-target activity in diabetic rats. We reasoned that if TTA-P2-

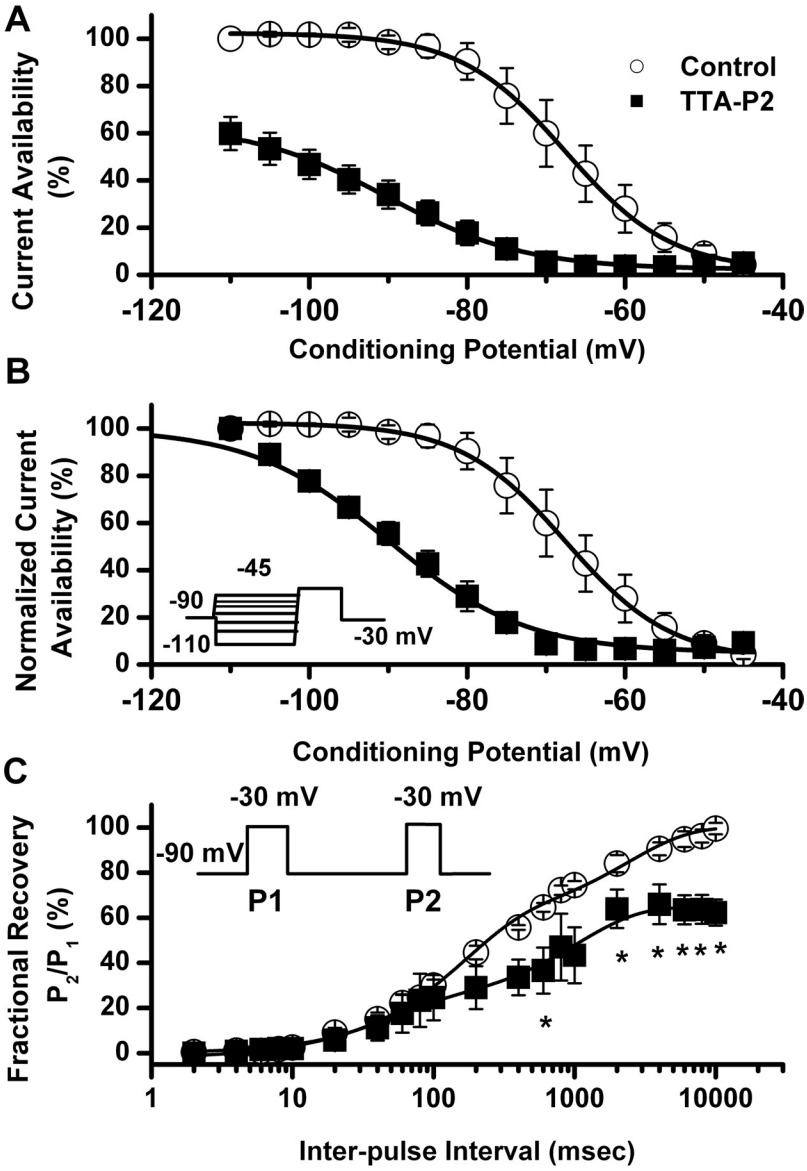

Fig. 5. Effects of TTA-P2 on steady-state inactivation and recovery from inactivation of T currents in rat DRG cells. A, current availability curves at different conditioning potentials before and during application of 100 nM TTA-P2 to the same cells. B, the same data are normalized for clarity of presentation in the lower panel of this figure ($n = 4$ cells). Open symbols represent the control conditions; filled symbols represent the conditions during bath application of TTA-P2. Solid black lines are fitted using eq. 3 (see *Materials and Methods*), giving half-maximal availability (V_{50}), which occurred at -67.5 ± 0.3 mV with a slope k of 6.7 ± 0.3 mV in control conditions. In contrast, fitted V_{50} was -90 ± 1 mV with a k of 8.7 ± 1.0 mV in the conditions when TTA-P2 was applied. Vertical lines represent S.E.M. of multiple determinations. Inset, voltage-clamp protocol. C, TTA-P2 impairs recovery from inactivation in DRG cells. Symbols on the graph indicate averaged data from multiple cells ($n = 5$), and solid lines were fitted with a double-exponential equation (eq. 5; see *Materials and Methods*); yielding in predrug control: $\tau 1$, 2388 ± 300 ms; $\tau 2$, 155 ± 15 ms; TTA-P2: $\tau 1$, 1045 ± 181 ms; $\tau 2$, 43 ± 15 ms. Note that in the presence of TTA-P2, currents recovered (P2/P1) only to approximately 60% of control current (*, $p < 0.05$). If the fitting curve in the presence of TTA-P2 was constrained to 100% recovery, we obtained the following recovery τ values: $\tau 1$, 16,130 ± 4316 ms; $\tau 2$, 165 ± 50 ms (data not shown). Inset, voltage-clamp protocol for our double-pulse protocol.

induced reversal of thermal hypersensitivity in diabetic rats is specifically mediated by the inhibition of T channels in vivo, then we should be able to abolish or at least greatly diminish any analgesic effects of TTA-P2 with knockdown of $Ca_V3.2$ in sensory neurons. Indeed, we found that pretreatment with specific AS against $Ca_V3.2$ in diabetic rats completely reversed diabetic hyperalgesia when given alone. When AS against $Ca_V3.2$ was administered concomitantly with TTA-P2 at 5, 7.5, or 10 mg/kg i.p., it did not significantly affect new baselines in either right or left paws (Fig. 7, bottom). In control experiments, we injected morphine (10 mg/kg i.p.) in AS- and MIS-treated diabetic rats and assessed its effect on thermal nociceptive responses at 1 h after injection. We found that morphine similarly decreased thermal nociceptive responses in both AS-treated (left paws, 7.2 ± 0.9 s; right paws, 7.4 ± 0.3 s increase in PWLs from baselines) and MIS-treated (left paws, 7.5 ± 0.4 s; right paws, 6.9 ± 0.9 s increase in PWLs from baselines) groups ($n = 3$ per group, $p > 0.05$, data not shown). This strongly suggests that abolished antihyperalgesic effect of TTA-P2 in AS-treated diabetic rats is not due to decreased basal pain responses. Diabetic rats did not appear to be less active than control ones despite some weight loss and severe hyperglycemia. Furthermore, although daily weights and blood glucose levels of rats treated with STZ and STZ+AS were different from baseline, they were not significantly different in the two treatment groups: baseline weight, 308 ± 7 g; STZ group, 280 ± 6 g; STZ+AS group, 275 ± 8 g; $n = 6$; baseline blood glucose, 84 ± 4 mg/dl; STZ group, 423 ± 39 mg/dl; STZ+AS group, 464 ± 40 mg/dl; $n = 6$. Thus, it appears that inhibition of $Ca_V3.2$ channels is the main mechanism that regulates TTA-P2-mediated antihyperalgesia in diabetic rats.

Discussion

In this study, we demonstrated that the new compound TTA-P2 is a potent and selective blocker of T currents in rat sensory neurons in vitro and a highly potent antinociceptive agent in two animal models of pain in vivo. The potency of TTA-P2 in inhibiting native DRG T current ($IC_{50} = 100$ nM) is close to that previously reported for inhibition of the re-

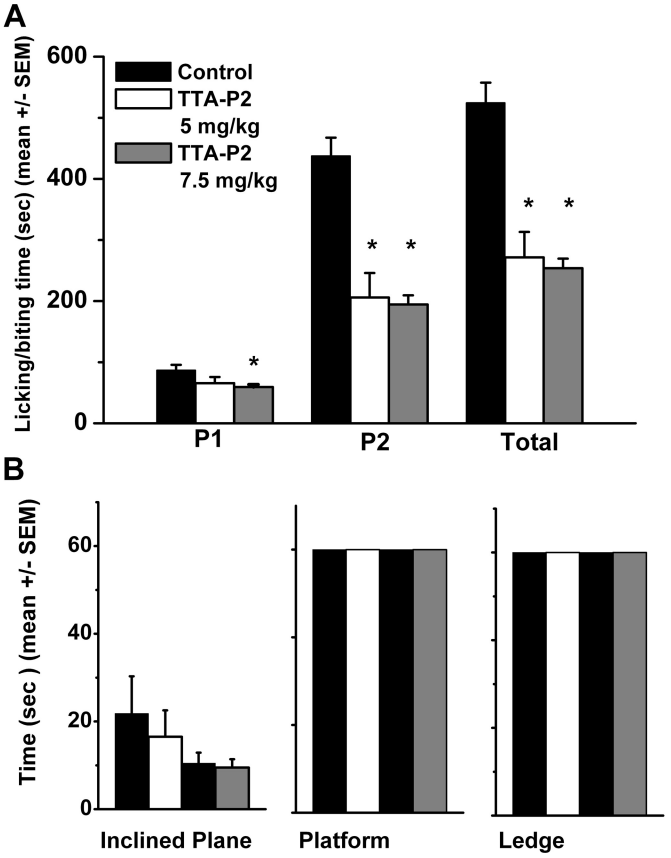

Fig. 6. TTA-P2 has antinocicpetive properties in the formalin pain model and has no effect on sensorimotor tests in mice. A, Adult mice experience significant analgesia after intraperitoneal injections of TTA-P2 at 5 mg/kg (open bars; $n = 8$) or 7.5 mg/kg (gray bars; $n = 14$) compared with experiments with vehicle (control, black bars; $n = 15$). Vertical bars indicate S.E.M.; the asterisks indicate a significance of $p < 0.01$ by Student's t test. B, histograms of average time in seconds in different sensorimotor tests using an inclined plane (left), platform (middle), and ledge (right) for mice given injections of 5 mg/kg TTA-P2 (white bars) or 7.5 mg/kg TTA-P2 (gray bars). Baseline measurements were taken 2 days before (controls, black bars). Note that black bars indicate controls with two different groups of animals receiving injections subsequently of either 5 or 7.5 mg/kg TTA-P2. Vertical bars indicate S.E.M. of multiple determinations. At either dose, TTA-P2 had no significant effect on either test, because $p > 0.05$ in comparisons of time points between controls and after injections of TTA-P2 ($n = 6$ mice in each group).

combinant Ca_V3 currents $Ca_V3.1$ (93 nM), $Ca_V3.2$ (196 nM), and $Ca_V3.3$ (84 nM) (Shipe et al., 2008). Indeed, we found that TTA-P2 in DRG cells even at 100-fold higher concentrations has little effect on other voltage-gated currents in sensory neurons. We also found that TTA-P2 inhibited DRG T currents in a voltage-dependent manner. Figure 4 summarizes our biophysical experiments, which indicate that TTA-P2 induced mild slowing of channel closure after brief depolarizations (deactivation), whereas it had a minimal effect on channel gating and macroscopic inactivation and activation rates.

It is noteworthy that the results shown in Fig. 5 indicate that TTA-P2 caused a marked voltage-dependent blockade of T channels, as demonstrated by a large hyperpolarizing shift of the steady-state inactivation curve. This voltage dependence indicates the drug's preference for inactive states of the channel, resulting in higher fractional block of the channel at depolarized membrane potentials. This is in contrast to mechanisms of inhibition in thalamic relay neurons in brain slices, where TTA-P2 acts as a state-independent antagonist of T channels (Dreyfus et al., 2010). However, it is possible that the difference between the mechanisms of channel inhibition in native thalamic and sensory neurons is due to the expression of different T-channel isoforms in thalamic relay neurons ($Ca_V3.1$) and DRG cells ($Ca_V3.2$). Our finding is somewhat unexpected, given that a previous study found that recombinant $Ca_V3.2$ channels were also inhibited by TTA-P2 in a voltage-independent manner (Shipe et al., 2008). In contrast, the structurally unrelated compound TTA-A2 shows state-dependent features of recombinant T-channel inhibition (Kraus et al., 2010). It is possible that different splice variants of $Ca_V3.2$ are expressed in adult DRG cells; alternatively, another unknown ancillary subunit that can modify the interaction of TTA-P2 with T channels may be coexpressed in DRG cells. It is noteworthy that we also have described substantial differences in the mechanism of T-channel blockade of native DRG cells and recombinant $Ca_V3.2$ channels for the anticonvulsants phenytoin and succinimide (Todorovic et al., 2000).

Additional molecular studies will be needed to resolve this issue. However, regardless of the precise basis for differences in the observations, voltage-dependent inhibition of the channel may be useful for clinical applications of TTA-P2, because it seems preferably to inhibit the neuronal excitability of actively firing DRG cells. This effect may explain the selective reversal of neuropathic hyperalgesia in diabetic rats with a dose that was completely ineffective in naive rats (Fig. 7). Thus, lowering the dose of drug used in vivo may greatly decrease the risk of adverse side effects. It is also important to note that some in vitro studies reported prominent expression of $Ca_V3.2$ T currents in non-nociceptive subpopulations of putative mechanosensitive DRG cells (Dubreuil et al., 2004; Coste et al., 2007). However, to our knowledge, the role of T channels in mechanosensation has not been validated in vivo.

The analgesic effect of TTA-P2 in the formalin inflammatory pain model in mice and antihyperalgesic effect in diabetic rats are achieved at concentrations of 5 to 10 mg/kg (Figs. 6 and 7). Previous pharmacokinetic studies in rodents and other species have shown that at these doses of plasma concentrations of TTA-P2 reach 0.2 to 1.0 μM and that TTA-P2 penetrates well into the CNS (Shipe et al., 2008). These findings strongly suggest that the analgesic and antihyperalgesic effects of TTA-P2 observed in our study could be related to the pharmacological antagonism of T currents in peripheral sensory neurons, the CNS, or both. It is noteworthy that we directly implicated the $Ca_V3.2$ isoform of T channels in the effects of TTA-P2 in diabetic neuropathic pain by demonstrating that injections of antisense oligonucleotides specific for $Ca_V3.2$ completely abolished effects of TTA-P2 on thermal PWLs (Fig. 7).

Our study strongly suggests that TTA-P2 is more suitable for functional studies than are many currently available compounds thought to be selective T-channel blockers. By virtue of their unique activation, deactivation, and inactivation properties, T currents are relatively easy to study in vitro in isolation from other calcium current components. However, pharmacological tools for identifying and investigating T currents have been very limited. For example, it was reported that a scorpion toxin, kurtoxin, potently blocks recombinant T currents at nanomolar

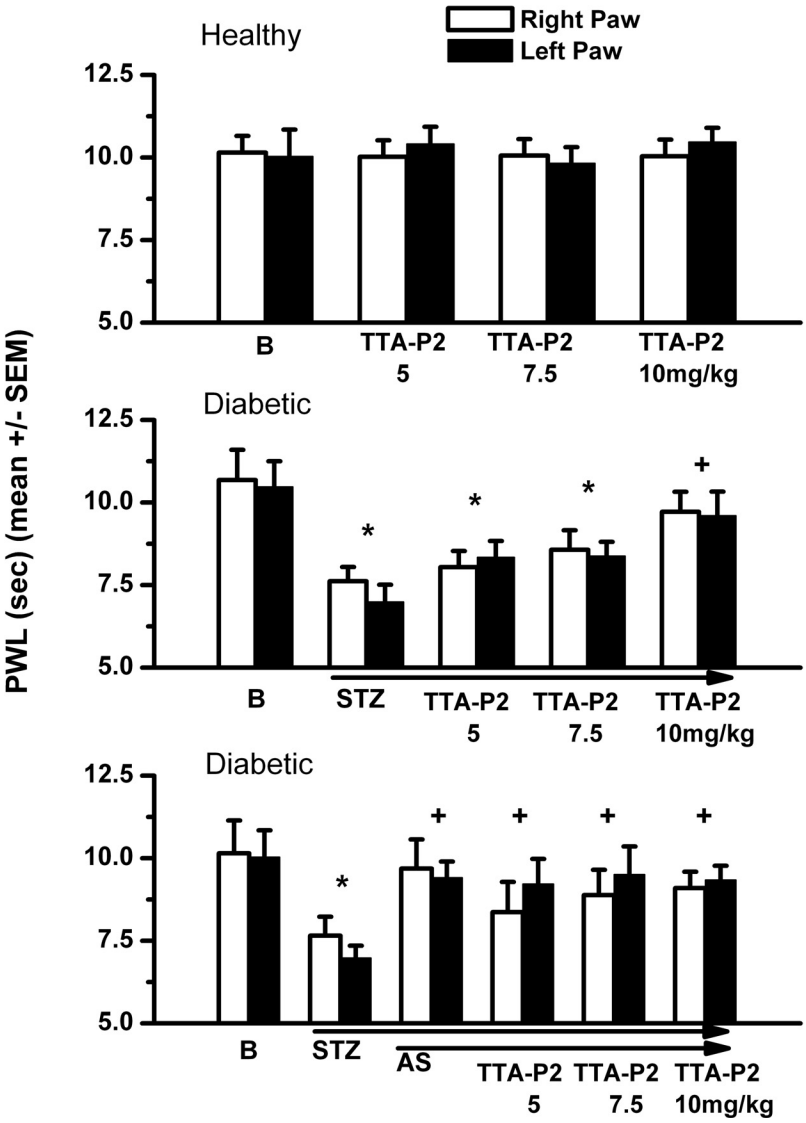

Fig. 7. TTA-P2 effectively reverses hyperalgesia in diabetic STZ-treated rats but does not change baseline nociceptive thresholds in healthy rats. Top, baseline (B) PWLs in right paws (open bars) and left paws (filled bars) remain stable 1 h after intraperitoneal injections of TTA-P2 at 5, 7.5, or 10 mg/kg. Middle, dose-dependent antihyperalgesic effect of TTA-P2, which, at 10 mg/kg i.p., completely reversed thermal hyperalgesia in STZ-treated diabetic rats. Bottom, note that AS treatment also completely reversed diabetic hyperalgesia, as indicated by the apparent normalization of PWLs, and that subsequent applications of TTA-P2 at different doses did not change PWLs. Vertical bars indicate S.E.M. of multiple experiments ($n = 4–8$ per group). $*$, $p < 0.05$ baseline (B) versus treatment at different doses of TTA-P2; $^{+}$, $p < 0.05$ for treatment with TTA-P2 versus new baseline in diabetic rats (STZ).

range with an IC_{50} for $Ca_V3.1$ of 15 nM (Chuang et al., 1998). However, kurtoxin has limited usefulness because it also blocks voltage-gated Na^+ currents and native HVA currents within the same concentration range (Chuang et al., 1998; Sidach and Mintz 2002). Of the other described compounds with known effects on T currents, including traditional agents such as ethosuximide (Coulter et al., 1989) and amiloride (Tang et al., 1988), most are reported to block with an IC_{50} in excess of 100 μM. At these concentrations, effects on other ion channels also occur, raising questions about the usefulness of these agents as specific probes of T-current function. Among the other available pharmacological agents, nickel at low micromolar concentrations (Lee et al., 1999b) and gaseous anesthetic/analgesic nitrous oxide up to 80% (Todorovic et al., 2001) can be used for selective definition of $Ca_V3.2$ T currents as opposed to other Ca_V3 currents. However, at similar concentrations, nickel blocks $Ca_V2.3$ *R*-type HVA currents (Zamponi et al., 1996), whereas nitrous oxide inhibits *N*-methyl-D-aspartate receptors in the CNS (Jevtovic-Todorovic et al., 1998).

Some new experimental agents are more promising in selectively targeting T channels. We have previously reported that a neuroactive steroid with a 5α configuration at the steroid A,B ring fusion [(+)-ECN] is a potent, voltage dependent, but only a partial blocker of T channels in rat sensory neurons (IC_{50} = 300 nM; maximal block, 40%) (Todorovic et al., 1998). In addition, we recently described another novel steroid, a voltage-dependent blocker of T channels in rat sensory neurons; it has a 5β configuration at the steroid A,B ring fusion ([(3β,5β,17β)-3-hydroxyandrostane-17-carbonitrile]), which more completely blocks T currents, but with decreased potency with an IC_{50} of 2.8 μM (Todorovic et al., 2004). Moreover, our previous studies have documented that both ECN and [(3β,5β,17β)-3-hydroxyandrostane-17-carbonitrile] are approximately 10-fold more potent in inhibiting T-type currents than in inhibiting HVA currents in rat sensory neurons (Todorovic et al., 1998, 2004). Compared with neuroactive steroids, it seems that TTA-P2 is even more potent and more selective in inhibiting T currents in DRG cells and thus is a better tool for the study of these channels. Although no preclinical data are currently available on the long-term use of ECN and related neuroactive steroids, evaluation of the

safety of TTA compounds in dogs has disclosed no cardiovascular or renal side effects (Shipe et al., 2008).

This study confirms our previously published conclusion that T-channel blockers are important and novel agents for the treatment of pain disorders. No presently available treatments can completely reverse the significantly adverse effects of intractable pain on quality-of-life measures. We hope that our studies may inspire future clinical trials that will lead to better treatments for intractable inflammatory pain and, in particular, the painful symptoms of patients with peripheral diabetic neuropathy.

Acknowledgments

We thank Damir Bojadzic for technical assistance and Dr. Toni Schneider for providing stable cell lines expressing $Ca_V2.3\beta3$ subunits. We thank Drs. Victor N. Uebele and John J. Renger for providing the TTA-P2 compound, supporting the experimental design, and reviewing this manuscript.

Authorship Contributions

Participated in research design: Choe, Messinger, Salajegheh, Jevtovic-Todorovic, and Todorovic.

Conducted experiments: Choe, Messinger, Leach, Eckle, Obradovic, and Salajegheh.

Performed data analysis: Messinger, Leach, Obradovic, and Todorovic.

Wrote or contributed to the writing of the manuscript: Jevtovic-Todorovic and Todorovic.

References

Aley KO and Levine JD (2001) Rapid onset pain induced by intravenous streptozotocin in the rat. *J Pain* **2:**146–150.

Bourinet E, Alloui A, Monteil A, Barrère C, Couette B, Poirot O, Pages A, McRory J, Snutch TP, Eschalier A, et al.(2005) Silencing of the $Ca_v3.2$ T-type calcium channel gene in sensory neurons demonstrates its major role in nociception. *EMBO J* **24:**315–324.

Campbell JN and Meyer RA (2006) Mechanisms of neuropathic pain. *Neuron* **52:**77–92.

Choi S, Na HS, Kim J, Lee J, Lee S, Kim D, Park J, Chen CC, Campbell KP, and Shin HS(2007) Attenuated pain responses in mice lacking Ca(V)3.2 T-type channels. *Genes Brain Behav* **6**:425–431.

Chuang RS, Jaffe H, Cribbs L, Perez-Reyes E, and Swartz KJ (1998) Inhibition of T-type voltage-gated calcium channels by a new scorpion toxin. *Nat Neurosci* **1:**668–674.

Clozel JP, Ertel EA, and Ertel SI (1997) Discovery and main pharmacological properties of mibefradil (Ro 40-5967), the first selective T-type calcium channel blocker. *J Hypertens Suppl* **15:**S17–S25.

Coste B, Crest M, and Delmas P (2007) Pharmacological dissection and distribution of NaN/Nav1.9, T-type Ca2+ currents, and mechanically activated cation currents in different populations of DRG neurons. *J Gen Physiol* **129:**57–77.

Coulter DA, Huguenard JR, and Prince DA (1989) Characterization of ethosuximide reduction of low-threshold calcium current in thalamic neurons. *Ann Neurol* **25:** 582–593.

Cribbs LL, Lee JH, Yang J, Satin J, Zhang Y, Daud A, Barclay J, Williamson MP, Fox M, Rees M, et al. (1998) Cloning and characterization of α1H from human heart, a member of the T-type Ca^{2+} channel gene family. *Circ Res* **83:**103–109.

Dib-Hajj SD, Fjell J, Cummins TR, Zheng Z, Fried K, LaMotte R, Black JA, and Waxman SG (1999) Plasticity of sodium channel expression in DRG neurons in the chronic constriction injury model of neuropathic pain. *Pain* **83:**591–600.

Dogrul A, Gardell LR, Ossipov MH, Tulunay FC, Lai J, and Porreca F (2003) Reversal of experimental neuropathic pain by T-type calcium channel blockers. *Pain* **105:**159–168.

Dreyfus FM, Tscherter A, Errington AC, Renger JJ, Shin HS, Uebele VN, Crunelli V, Lambert RC, and Leresche N (2010) Selective T-type calcium channel block in thalamic neurons reveals channel redundancy and physiological impact of I(T)window. *J Neurosci* **30:**99–109.

Dubreuil AS, Boukhaddaoui H, Desmadryl G, Martinez-Salgado C, Moshourab R, Lewin GR, Carroll P, Valmier J, and Scamps F (2004) Role of T-type calcium current in identified D-hair mechanoreceptor neurons studied *in vitro*. *J Neurosci* **24:**8480–8484.

Edwards JL, Vincent AM, Cheng HT, and Feldman EL (2008) Diabetic neuropathy: mechanisms to management. *Pharmacol Ther* **120:**1–34.

Hong S, Morrow TJ, Paulson PE, Isom LL, and Wiley JW (2004) Early painful diabetic neuropathy is associated with differential changes in tetrodotoxin-sensitive and -resistant sodium channels in dorsal root ganglion neurons in the rat. *J Biol Chem* **279:**29341–29350.

Institute of Laboratory Animal Resources (1996) *Guide for the Care and Use of Laboratory Animals* 7th ed. Institute of Laboratory Animal Resources, Commission on Life Sciences, National Research Council, Washington DC.

Jagodic MM, Pathirathna S, Nelson MT, Mancuso S, Joksovic PM, Rosenberg ER, Bayliss DA, Jevtovic-Todorovic V, and Todorovic SM (2007) Cell-specific alterations of T-type calcium current in painful diabetic neuropathy enhance excitability of sensory neurons. *J Neurosci* **27:**3305–3316.

Jevtovic-Todorovic V, Todorović SM, Mennerick S, Powell S, Dikranian K, Benshoff N, Zorumski CF, and Olney JW (1998) Nitrous oxide (laughing gas) is an NMDA antagonist, neuroprotectant and neurotoxin. *Nat Med* **4:**460–463.

Jevtovic-Todorovic V and Todorovic SM (2006) The role of peripheral T-type calcium channels in pain transmission. *Cell Calcium* **40:**197–203.

Kim D, Park D, Choi S, Lee S, Sun M, Kim C, and Shin HS (2003) Thalamic control of visceral nociception mediated by T-type Ca^{2+} channels. *Science* **302:**117–119.

Kraus RL, Li Y, Gregan Y, Gotter AL, Uebele VN, Fox SV, Doran SM, Barrow JC, Yang ZQ, Reger TS, et al. (2010) In vitro characterization of T-type calcium channel antagonist TTA-A2 and in vivo effects on arousal in mice. *J Pharmacol Exp Ther* **335:**409–417.

Lai J, Gold MS, Kim CS, Bian D, Ossipov MH, Hunter JC, and Porreca F (2002) Inhibition of neuropathic pain by decreased expression of the tetrodotoxin-resistant sodium channel, NaV1.8. *Pain* **95:**143–152.

Latham JR, Pathirathna S, Jagodic MM, Choe WJ, Levin ME, Nelson MT, Lee WY, Krishnan K, Covey DF, Todorovic SM, et al.(2009) Selective T-type calcium channel blockade alleviates hyperalgesia in ob/ob mice. *Diabetes* **58:**2656–2665.

Lee JH, Daud AN, Cribbs LL, Lacerda AE, Pereverzev A, Klöckner U, Schneider T, and Perez-Reyes E (1999a) Cloning and expression of a novel member of the low voltage-activated T-type calcium channel family. *J Neurosci* **19:**1912–1921.

Lee JH, Gomora JC, Cribbs LL, and Perez-Reyes E (1999b) Nickel block of three cloned T-type calcium channels: low concentrations selectively block alpha1H. *Biophys J* **77:**3034–3042.

Leresche N, Parri HR, Erdemli G, Guyon A, Turner JP, Williams SR, Asprodini E, and Crunelli V (1998) On the action of the anti-absence drug ethosuximide in the rat and cat thalamus. *J Neurosci* **18:**4842–4853.

Lory P and Chemin J (2007) Towards the discovery of novel T-type calcium channel blockers. *Expert Opin Ther Targets* **11:**717–722.

McCleskey EW and Gold MS (1999) Ion channels of nociception. *Annu Rev Physiol* **61:**835–856.

McGivern JG (2006) Pharmacology and drug discovery for T-type calcium channels. *CNS Neurol Disord Drug Targets* **5:**587–603.

Messinger RB, Naik AK, Jagodic MM, Nelson MT, Lee WY, Choe WJ, Orestes P, Latham JR, Todorovic SM, and Jevtovic-Todorovic V (2009) In vivo silencing of the Ca(V)3.2 T-type calcium channels in sensory neurons alleviates hyperalgesia in rats with streptozocin-induced diabetic neuropathy. *Pain* **145:**184–195.

Nakashima YM, Todorovic SM, Pereverzev A, Hescheler J, Schneider T, and Lingle CJ (1998) Properties of Ba^{2+} currents arising from human α_{1E} and $\alpha_{1E}\beta_3$ constructs expressed in HEK293 cells: physiology, pharmacology, and comparison to native T-type Ba^{2+} currents. *Neuropharmacology* **37:**957–972.

Nelson MT, Joksovic PM, Perez-Reyes E, and Todorovic SM (2005) The endogenous redox agent L-cysteine induces T-type Ca^{2+} channel-dependent sensitization of a novel subpopulation of rat peripheral nociceptors. *J Neurosci* **25:**8766–8775.

Nelson MT, Woo J, Kang HW, Vitko I, Barrett PQ, Perez-Reyes E, Lee JH, Shin HS, and Todorovic SM (2007) Reducing agents sensitize C-type nociceptors by relieving high-affinity zinc inhibition of T-type calcium channels. *J Neurosci* **27:**8250–8260.

Orestes P, Bojadzic D, Lee J, Leach E, Salajegheh R, Digruccio MR, Nelson MT, and Todorovic SM (2011) Free radical signalling underlies inhibition of CaV3.2 T-type calcium channels by nitrous oxide in the pain pathway. *J Physiol* **589:**135–148.

Perez-Reyes E (2003) Molecular physiology of low-voltage-activated T-type calcium channels. *Physiol Rev* **83:**117–161.

Perez-Reyes E, Cribbs LL, Daud A, Lacerda AE, Barclay J, Williamson MP, Fox M, Rees M, and Lee JH (1998) Molecular characterization of a neuronal low-voltage-activated T-type calcium channel. *Nature* **391:**896–900.

Randall AD and Tsien RW (1997) Contrasting biophysical and pharmacological properties of T-type and R-type calcium channels. *Neuropharmacology* **36:**879–893.

Rogawski MA and Löscher W (2004) The neurobiology of antiepileptic drugs for the treatment of nonepileptic conditions. *Nat Med* **10:**685–692.

Shipe WD, Barrow JC, Yang ZQ, Lindsley CW, Yang FV, Schlegel KA, Shu Y, Rittle KE, Bock MG, Hartman GD, et al. (2008) Design, synthesis, and evaluation of a novel 4-aminomethyl-4-fluoropiperidine as a T-type Ca^{2+} channel antagonist. *J Med Chem* **51:**3692–3695.

Sidach SS and Mintz IM (2002) Kurtoxin, a gating modifier of neuronal high- and low-threshold ca channels. *J Neurosci* **22:**2023–2034.

Snutch TP and David LS (2005) T-type calcium channels: an emerging therapeutic target for the treatment of pain. *Drug Dev Res* **67:**404–415.

Tang CM, Presser F, and Morad M (1988) Amiloride selectively blocks the low threshold (T)-type calcium channel. *Science Wash DC* **240:**213–215.

Todorovic SM, Jevtovic-Todorovic V, Meyenburg A, Mennerick S, Perez-Reyes E, Romano C, Olney JW, and Zorumski CF (2001) Redox modulation of T-type calcium channels in rat peripheral nociceptors. *Neuron* **31:**75–85.

Todorovic SM and Lingle CJ (1998) Pharmacological properties of T-type Ca^{2+} current in adult rat sensory neurons: effects of anticonvulsant and anesthetic agents. *J Neurophysiol* **79:**240–252.

Todorovic SM, Meyenburg A, and Jevtovic-Todorovic V (2002) Mechanical and thermal antinociception in rats following systemic administration of mibefradil, a T-type calcium channel blocker. *Brain Res* **951:**336–340.

Todorovic SM, Meyenburg A, and Jevtovic-Todorovic V (2004a) Redox modulation of peripheral T-type Ca^{2+} channels in vivo: alteration of nerve injury-induced thermal hyperalgesia. *Pain* **109:**328–339.

Todorovic SM, Pathirathna S, Brimelow BC, Jagodic MM, Ko SH, Jiang X, Nilsson KR, Zorumski CF, Covey DF, and Jevtovic-Todorovic V (2004b) 5β-Reduced neuroactive steroids are novel voltage-dependent blockers of T-type Ca2+ channels in rat sensory neurons in vitro and potent peripheral analgesics in vivo. *Mol Pharmacol* **66:**1223–1235.

Todorovic SM, Perez-Reyes E, and Lingle CJ (2000) Anticonvulsants but not general

anesthetics have differential blocking effects on different T-type current variants. *Mol Pharmacol* **58:**98–108.
Todorovic SM, Prakriya M, Nakashima YM, Nilsson KR, Han M, Zorumski CF, Covey DF, and Lingle CJ (1998) Enantioselective blockade of T-type Ca2+ current in adult rat sensory neurons by a steroid that lacks gamma-aminobutyric acid-modulatory activity. *Mol Pharmacol* **54:**918–927.
Todorovic SM, Rastogi AJ, and Jevtovic-Todorovic V (2003) Potent analgesic effects of anticonvulsants on peripheral thermal nociception in rats. *Br J Pharmacol* **140:**255–260.
Zamponi GW, Bourinet E, and Snutch TP (1996) Nickel block of a family of neuronal calcium channels: subtype- and subunit-dependent action at multiple sites. *J Membr Biol* **151:**77–90.

Address correspondence to: Slobodan M. Todorovic, Department of Anesthesiology, University of Virginia Health System, Mail Box 800710, Charlottesville, VA 22908-0710. E-mail: st9d@virginia.edu